

**SOMATIC HYBRIDIZATION PROVIDES SEGREGATING POPULATIONS
FOR THE IDENTIFICATION OF CAUSATIVE MUTATIONS IN STERILE
MUTANTS OF THE MOSS *PHYSCOMITRELLA PATENS***

**Laura A. Moody¹, Steven Kelly¹, Yoan Coudert^{2,4}, Zachary L. Nimchuk³, C. Jill Harrison² &
Jane. A. Langdale¹**

¹ Department of Plant Sciences, University of Oxford, South Parks Road, Oxford, OX1 3RB, UK

² School of Biological Sciences, Life Sciences Building, University of Bristol, 24 Tyndall Avenue, Bristol BS8 1TQ, UK

³ UNC Department of Biology, Coker Hall, 120 South Road, Chapel Hill, NC 27599-3280, USA

⁴ Laboratoire Reproduction et Développement des Plantes, Ecole Normale Supérieure de Lyon, CNRS, INRA, Université Claude Bernard Lyon 1, 46 Allée d'Italie, 69007 Lyon, France

Author for correspondence: jane.langdale@plants.ox.ac.uk

SUMMARY

- Forward genetics is now straightforward in the moss *Physcomitrella patens*, and large mutant populations can be screened relatively easily. However, perturbation of development prior to the formation of gametes currently leaves no route to gene discovery.
- Somatic hybridization has previously been used to rescue sterile mutants and to assign *P. patens* mutations to complementation groups, but the cellular basis of the fusion process could not be monitored, and there was no tractable way to identify causative mutations.
- Here we use fluorescently tagged lines to generate somatic hybrids between Gransden (Gd) and Villersexel (Vx) strains of *P. patens*, and show that hybridization produces fertile diploid gametophytes that form phenotypically normal tetraploid sporophytes. Quantification of genetic variation between the two parental strains reveals single nucleotide polymorphisms at a frequency of 1/286 bp.
- Given that the genetic distinction between Gd and Vx strains exceeds that found between pairs of strains that are commonly used for genetic mapping in other plant species, the spore populations derived from hybrid sporophytes provide suitable material for bulk segregant analysis and gene identification by genome sequencing.

KEYWORDS

Gene discovery; fluorescent tagged lines; forward genetics; protoplast fusion; *Physcomitrella patens*.

INTRODUCTION

The release of the *P. patens* genome sequence over a decade ago provided new opportunities to address fundamental questions about land plant evolution and development at the molecular level (Rensing *et al.*, 2008). Since homologous recombination can be directed in *P. patens* at a similar efficiency to the yeast *Saccharomyces cerevisiae*, reverse genetic analysis via gene targeting is both straightforward and commonly reported (Schaefer & Zrýd, 2001; Cove *et al.*, 2006). Furthermore, *P. patens* has a predominantly haploid life cycle, which means that transgenic lines can be generated rapidly, without a requirement for backcrossing (Reski & Frank, 2005; Cove *et al.*, 2006). Comparative genomics and reverse genetic approaches have thus played a significant role in determining gene function in *P. patens* and have allowed ancestral roles for a number of genes to be inferred (Yasumura *et al.*, 2007, 2005; Hirano *et al.*, 2007; Menand *et al.*, 2007; Ludwig-Muller *et al.*, 2009; Mosquna *et al.*, 2009; Chater *et al.*, 2011; Bennett *et al.*, 2014; Perroud *et al.*, 2014; Sakakibara *et al.*, 2014; Horst *et al.*, 2016).

In contrast to reverse genetic approaches, forward genetics represents an unbiased and powerful strategy to uncover previously unknown regulators of developmental processes. Forward genetic studies in *P. patens* were first described in the literature over 40 years ago, with mutants typically generated by treating spores with either N-methyl-N'-nitro-N-nitrosoguanidine (NTG) or Ethyl Methane Sulphonate (EMS) (Ashton *et al.*, 1979a,b). The mutants described were predominantly auxotrophic in nature or exhibited impaired responses to the phytohormones auxin and cytokinin (Ashton & Cove, 1977; Grimsley *et al.*, 1977a; Ashton *et al.*, 1979a,b). The mapping of causative mutations was rare (Courtice *et al.*, 1978), partly due to the inability to distinguish between sporophytes derived from self-fertilization and those derived from outcrossing. Downstream diagnostics were therefore laboured, making forward genetics in *P. patens* an unappealing prospect for many. Although shuttle- and transposon-based methods were subsequently developed, both were labour-intensive and were not widely adopted by the research community (Nishiyama, 2000; Egner *et al.*, 2002). A large sequence-indexed library of T-DNA insertion mutations in the *P. patens* genome was screened with some success (Cove *et al.*, 2009a; Vives *et al.*, 2016) but even with this resource, very few genes have been identified in *P. patens* through forward genetic approaches (Prigge *et al.*, 2010; Saruhashi *et al.*, 2015; Stevenson *et al.*, 2016b).

Within the last decade, forward genetics in *P. patens* has become more tractable, not least through the identification of the Villersexel (Vx) strain, which can be crossed to the original Gransden (Gd) strain used by most research groups (von Stackelberg *et al.*, 2006; Stevenson *et al.*, 2016a). The construction of a genetic map (Kamisugi *et al.*, 2008), the development of a UV-mediated mutagenesis method for protoplasts (Cove & Quatrano, 2006; Stevenson *et al.*, 2016a), and the generation of fluorescent marker lines (e.g. Gd::GFP and Vx::mCherry) that can be used as visual tools for identifying hybrid sporophytes (Perroud *et al.*, 2011) have all contributed to the ease with which forward genetics can now be carried out in *P. patens*. However, a major obstacle remains in that many mutants are reproductively impaired due to failures in gametophore development or gametangium formation. Although somatic hybridization techniques can overcome these barriers to enable sexual propagation of mutant lines, technological limitations have thus far prevented identification of causative mutations, allowing only mutant assignment to complementation groups (Grimsley *et al.*, 1977a,b; Ashton *et al.*, 1979b; Featherstone *et al.*, 1990). A candidate gene approach allowed identification of the causative mutations in classical auxin resistant mutants (Ashton *et al.*, 1979a; Prigge *et al.*, 2010) but this approach would not be feasible in mapping traits where the genetic basis is unknown. Here we report a method that can be used to map causative mutations in sterile mutants. The method, which combines somatic hybridization with bulk segregant analysis, was optimized using fluorescent reporter lines (both existing and newly generated) which allowed the cellular changes that occur during protoplast

fusion and the formation of somatic hybrids to be monitored. The feasibility of the method for genetic mapping was demonstrated through quantification of the genome-wide genetic variation between Gd and Vx strains. Adoption of this methodology in forward genetic screens of *P. patens* will facilitate the dissection of aspects of growth and development that have thus far been intractable.

MATERIALS AND METHODS

Plant material and growth conditions

The Gransden (Gd) (Engel, 1968) and Villersexel (Vx) strains of *Physcomitrella patens* subsp. *patens*, all marker lines, and somatic hybrids were grown and maintained under sterile conditions on BCD or BCDAT medium (Nishiyama, 2000) at 24 °C with a 16 h : 8 h, light (300 $\mu\text{mol m}^{-2} \text{s}^{-1}$): dark cycle. For sporophyte induction in both haploid and diploid lines, 1-week-old protonemal tissue was transferred into Magenta pots containing 100 ml solidified BCD medium supplemented with 1 mM CaCl_2 , and grown at 24 °C for 6 weeks with a 16 h : 8 h, light (300 $\mu\text{mol m}^{-2} \text{s}^{-1}$): dark cycle. Magenta pots were then transferred to 16 °C, with an 8 h : 16 h light (150 $\mu\text{mol m}^{-2} \text{s}^{-1}$) : dark cycle. Sterile water was added immediately after transfer to 16 °C and sporophytes were harvested after approximately 3-6 months.

Generation of fluorescent reporter lines

A plasma membrane-targeted YPet (Nguyen & Daugherty, 2005) construct was generated by recombinant PCR (Horton *et al.*, 2013) using the following four primers:

- 1) 29-1Fwd: ccggatccATGAGTACAGCTACTTTCGTTGATATTATTATC
- 2) 29-1linkerR: cagccatggatcgggctgccgcagcggcagcagccgcagcaggTTTGGTGAGGACATAAATGGC
- 3) 29-1linkerF:GCCATTTATGTCCTCACCAAACctgctgcggctgctgccgctgcggcagcccgatccatggctg
- 4)YPet BH1rvs: gggatcctaTTTGTACAATTCATTCATACCCTCGG

In a first round of PCR, primers 1 & 2 were used to amplify the 29-1 plasma membrane targeting sequence from Arabidopsis Col-0 DNA, and primers 3 & 4 were used to amplify YPet from a plasmid template. In a second round of PCR, primers 1 and 4 were used for amplification using the products from round 1 as template DNA. The resultant fragment was cloned into pCR2.1, sequenced, and released by BamHI digestion prior to insertion into a *pUBQ::FPOcs* expression cassette constructed in pBJ36 (Eshed *et al.*, 2001). The expression cassette was released by AscI/NotI digestion and cloned into p108 (Bezanilla *et al.*, 2005) for targeted insertion into the *P. patens* genome. Wild-type Gransden 2004 protoplasts were transformed using the polyethylene glycol-based transformation method (Schaefer *et al.*, 1991), and following two rounds of antibiotic selection, lines were screened by fluorescence.

Somatic hybridization and segregation analysis

Somatic hybridization between different transgenic marker lines was carried out using the polyethylene glycol-based method, with minor modifications (Cove *et al.*, 2009b). 1 % Driselase (Sigma-Aldrich #D8037) was prepared in 8 % mannitol, incubated at room temperature for 15 min with gentle agitation, centrifuged for 3 min at 3,300 x g and then filter-sterilized (pellet discarded). Protonemata that had been grown on cellophane-overlaid BCDAT medium, were harvested and added to 1 % Driselase (in 8 % mannitol) and incubated, with gently agitation, for 40 min. The cell suspension was filtered through a sterile 40 µm cell strainer (Fisher Scientific #10737821) into a 14 ml round bottomed tube (Fisher Scientific #10568531) and then centrifuged for 3 min at 120 x g at room temperature with no braking. Cells were washed twice using 6 ml 8 % mannitol and then resuspended in 6 ml 8 % mannitol at a final cell density of 1×10^6 cells ml⁻¹. 1 ml of each cell suspension (1×10^6 cells total) were combined, mixed gently and then centrifuged for 3 min at 120 x g at room temperature with no braking. Protoplasts were resuspended in 250 µl PW solution (10 mM CaCl₂ and 8.5 % mannitol). Somatic hybridization was initiated by adding 750 µl PEG/F (5 mM CaCl₂ and 50 % PEG 6000 (w/v)) and mixing gently. After 40 min, 1.5 ml of PW solution was added. After 50 min, another 10 ml of PW solution was added. After 60 min, a further 10 ml of PW solution was added. Following each addition of PW solution, protoplasts were mixed gently. After 70 min, protoplasts were centrifuged at 120 x g for 3 min at room temperature with no braking.

To visualize fusion events in protoplasts, between NLS-GFP and PM-YPet lines, pellets were resuspended in 6 ml liquid BCDAT supplemented with 10 mM CaCl₂, 8 % mannitol and 1 % glucose (BCDATG) and kept in the dark for 24 h in standard growth conditions. Cell suspensions were then centrifuged at 120 x g for 3 min at room temperature with no braking. The majority of BCDATG medium was removed, leaving enough (~200 µl) to transfer the cells to a microscope slide. Successful fusion events were monitored by scanning all of the surviving protoplasts under the confocal microscope.

To select for stable Vx::mCherry/Gd::mGFP hybrids, pellets were immediately resuspended in 4 ml 8 % mannitol and then 1 ml was plated onto cellophane-overlaid BCDATG medium. Plates were kept in the dark for 48 h and then transferred to standard growth conditions. After one week, cellophane discs were removed and then transferred to BCDAT medium supplemented with both 50 µgml⁻¹ G418 and 20 µgml⁻¹ hygromycin B, to select for stable hybrids.

Sporophyte production was induced as described above. Spores were germinated on spore germination medium and allowed to grow for a period of two weeks. Sporelings were then transferred

to individual wells of a 24-well tissue culture plate containing BCD medium for one month. To carry out segregation analysis of progeny produced from Vx::mCherry/Gd::GFP diploid hybrids, individuals were replica plated onto BCD medium containing either 50 $\mu\text{g ml}^{-1}$ G418 or 20 $\mu\text{g ml}^{-1}$ hygromycin B and grown for two weeks when viability could be determined.

Microscopy

Fluorescence microscopy was carried out with a Zeiss LSM510 META confocal microscope (ZEISS). A 40x water immersive lens (C-Apochromat 40x/1.20 W) was used for all imaging. mGFP was excited with the 458 nm laser line and detected with a 475-525 nm bandpass filter. YPet was excited with the 514 nm laser line and detected with a 535-591 IR bandpass filter. mCherry was excited with the 543 nm laser line and detected with a 585-615 bandpass filter. Protoplasts were mounted onto slides in osmotically controlled liquid BCD and plant material was mounted onto slides in sterile water. Other images were captured using a Leica M165C microscope equipped with a Qimaging Micropublishing 5.0 RTV camera.

Sequencing, read processing and variant calling

Total genomic DNA was isolated from one week old protonemata maintained on cellophane-overlaid BCDAT medium using the CTAB method (Yasumura *et al.*, 2005). Genomic DNA was extracted from both Vx::mCherry and Gd::GFP parental lines to identify SNPs that distinguished the two marker strains. DNA samples (~3 μg) were sequenced using an Illumina HiSeq4000 platform (150 bp PE read lengths) at the Wellcome Trust Centre for Human Genetics, University of Oxford. Raw reads were quality controlled using Trimmomatic (Bolger *et al.*, 2014) with settings LEADING:20 TRAILING:20 SLIDINGWINDOW:5:20 MINLEN:50. Read libraries were mapped to the *P. patens* genome (Version Ppatens_318_v3 obtained from Phytozome V11) using BWA-MEM (Li, 2013). After removing duplicate mapped reads and realigning mapped reads around indels, variants were called according to best practice guidelines from GATK using GATK v3.6 (McKenna *et al.*, 2012). All indels and single nucleotide variants identified as low quality by GATK were discarded. Nucleotide positions where the Gd strain was identical to the genome reference and the Vx strain was different (with a maximum likelihood allele frequency of 1.0) were selected as strain distinguishing variants. The supplementary tab delimited text file contains the three columns which comprise the chromosome position and the variant nucleotide (Supplementary File S2).

RESULTS AND DISCUSSION

To visualize the cellular changes that occur during the process of somatic hybridization, a *P. patens* line was generated that constitutively expresses a plasma membrane localized YPet from the maize ubiquitin promoter (Fig. S1). Somatic hybrids were generated between protoplasts isolated from the YPet line (PM-YPet) and protoplasts isolated from a line that accumulates nuclear localized green fluorescent protein (NLS-GFP) (Bezanilla *et al.*, 2003) (Fig. 1a). Following cellular fusion, four different classes of hybrids were identified: NLS-GFP/NLS-GFP (Fig. 1b) and PM-YPet/PM-YPet (Fig. 1c) homodikaryons that contained two genetically identical nuclei within a single fused protoplast; NLS-GFP/PM-YPet heterodikaryons that contained two genetically distinct nuclei within a single fused protoplast (Fig. 1d); and homotrikaryons containing three identical NLS-GFP/NLS-GFP or heterotrikaryons with three distinct NLS-GFP/PM-YPet nuclei (data not shown). NLS-GFP/NLS-GFP homodikaryons and NLS-GFP/PM-YPet heterodikaryons were detected at equal frequencies to one another and trikaryons were detected more rarely (approximately 1/10 total hybrids).

Having established that heterodikaryons could be produced at high frequency, we then tested whether stable somatic hybrids could be generated between the Gd and Vx strains of *P. patens*. Using the single insertion Gd::GFP and Vx::mCherry fluorescent marker lines that are already widely utilized and available to the global scientific community (Perroud *et al.*, 2011), protoplasts were fused and hybrids were regenerated on osmotically controlled medium containing both G418 and hygromycin. Stable hybrid lines that constitutively expressed both GFP and mCherry were obtained, with Gd::GFP/Vx::mCherry synkaryons containing chromosomes from both haploid parents enveloped within a single nucleus. At an undetermined stage during the protoplast regeneration process, nuclear fusion had occurred (Fig. 2a). Approximately 37% of the hybrids produced very few gametophores and were reproductively sterile, resembling Class III hybrids described previously (Grimsley *et al.*, 1977b). The remaining 63% of the Gd::GFP/Vx::mCherry hybrid lines more closely resembled the parental Gd::GFP and Vx::mCherry haploid lines (Fig. 3). Importantly, Gd::GFP/Vx::mCherry hybrid lines were reproductively viable. Following self-fertilization of these hybrid gametophytes, the presumed tetraploid sporophytes produced spores that constitutively expressed both GFP and mCherry (Fig. 2b).

Although life cycle completion in the hybrid lines took approximately three months longer than comparable Gd or Vx diploid sporophytes, fully viable spores were harvested. To check segregation ratios, spores from five of the Gd::GFP/Vx::mCherry hybrid lines were first germinated on

cellophane-overlaid spore germination medium. Regenerating sporelings were then replica plated onto medium supplemented with G418 or hygromycin and allowed to grow for a period of two weeks. The segregating progeny exhibited an antibiotic segregation ratio consistent with meiosis from an autotetraploid i.e. 5:25:5:1 – G418^R/Hyg^S:G418^R/Hyg^R:G418^S/Hyg^R:G418^S/Hyg^S (Table 1). All sporophytes were therefore derived from self-fertilized diploid gametophytes and produced viable diploid spores.

To determine whether sequence variability between the *P. patens* Gd and Vx strains is sufficient to enable the progeny of somatic hybrids to be used to map mutated loci, genomic DNA was isolated from both Gd::GFP and Vx::mCherry parental marker lines and sequenced on an Illumina sequencing platform. Comparison of the sequence data from the Gd::GFP and Vx::mCherry parental strains identified a set of 2,255,671 single nucleotide variants that distinguished the two strains. The median number of single nucleotide variants between the two strains was 35 per 10 kb, and this was consistent across all chromosomes (Fig. 4, Fig. S2). This variability between *P. patens* Gd and Vx strains is substantial, and is comparable to that observed between Ler and Col strains of *Arabidopsis* (29 per 10kb on average) that are commonly used for mapping (Lu et al., 2012).

Perroud *et al.* originally generated the Gd::GFP and Vx::mCherry marker lines to enable the detection of successful outcrossing events (Perroud *et al.*, 2011). However, we propose that the use of these lines, can be extended towards using forward genetics to study traits that would usually result in sterility, such as 3D growth, tip growth and embryo/sporophyte development. Firstly, a forward genetic screen would be carried out via UV-mediated mutagenesis of protoplasts isolated from the Vx::mCherry marker line, to identify mutants of interest (e.g. defective tip growth). Somatic hybridization would then be carried out between the sterile mutant in the Vx::mCherry background and the non-mutagenized Gd::GFP marker line. The resulting diploid hybrid will be reproductively competent and will produce a tetraploid sporophyte. The proportion of segregating diploid spore progeny that bear the original mutant phenotype will vary between 16.7% ('random chromosome segregation') and 21.4% ('random chromatid segregation'), depending on whether the gene of interest is linked to the centromere or not (Grimsley *et al.*, 1977b). By pooling genomic DNA from individuals bearing the original mutant phenotype (the mutant pool) and individuals with a wild type phenotype (the wild type pool), the causative recessive mutation could be identified by genome sequencing and comparison with genome sequence from the original parental marker lines (Gd::GFP, Vx::mCherry). There are two parameters to consider when designing such an experiment; the read depth that will be obtained and the number of individuals to be pooled for sequencing. The read depth

is important for determining resolution of allele frequencies but is constrained by the cost of whole genome re-sequencing. For example, a mean read depth of 2 gives a resolution of 0.5 (i.e. an allele frequency can be 0, 0.5 or 1) and a mean read depth of 100 gives a resolution of 0.01 (i.e. an allele frequency can be any multiple of 0.01 between 0 and 1). Typically, a read depth of >20X is considered an acceptable compromise between cost and resolution (i.e. a resolution of 0.05). Ideally, aiming for a read depth of ~30X will ensure that most sites in the genome would exceed 20X coverage. To ensure that allele frequencies obtained from sequencing the pooled samples are a reliable approximation of the frequency in the true population, the pool size should be sufficiently large that sequencing reads mapped to the same region of the genome originate from different individuals. The probability that two or more reads spanning any given base are sampled from the same individual in the pool can be calculated using the cumulative binomial distribution. Given an anticipated read depth of ~30X, selecting a pool size of 120 individuals (for both mutant and wild type pools) means that the probability that two or more reads spanning any given nucleotide would come from the same individual in the pool is 0.026. The feasibility of this experimental approach has recently been demonstrated (Moody *et al.*, 2018).

CONCLUSION

The ease of reverse genetic studies has greatly facilitated studies of gene function in *P. patens*. However, these candidate gene-driven approaches are limited by prior knowledge because they rely on findings from studies in other model plant species, usually *A. thaliana*. In contrast, forward genetic studies offer a powerful approach to unearth previously unknown genetic regulators of any given phenotype or trait. Frustratingly, forward genetics in *P. patens* has been hindered by a lack of suitable methods for mapping causative recessive mutations in sterile mutants, and consequently, many classical mutants remain uncharacterized. Here we have developed a strategy that can circumvent this problem, in that somatic hybridization can be combined with bulk segregant analysis for gene identification by genome sequencing. This technology has the potential to revolutionize studies of gene function in *P. patens*.

ACKNOWLEDGEMENTS

We are grateful to Pierre-François Perroud for providing the Vx::mCherry and Gd::GFP marker lines, and to Magdalena Bezanilla for the NLS-GFP line. The work was funded by ERC Advanced Investigator (EDIP) and BBSRC (BB/M020517/1) grants to JAL, and by The Queen's College Oxford Browne Fellowship and a Company of Biologists Travel Fellowship to CJH. SK was funded by a

Royal Society University Research Fellowship. We thank Elliot Meyerowitz for hosting CJH in his lab.

AUTHOR CONTRIBUTIONS

LAM carried out the somatic hybridization experiments; SK carried out the bioinformatics; YC, ZLN and CJH made the PM-YPet line; LAM, SK, CJH and JAL wrote the manuscript.

REFERENCES

- Ashton NW, Cove DJ. 1977.** The isolation and preliminary characterisation of auxotrophic and analogue resistant mutants of the moss, *Physcomitrella patens*. *Molecular & General Genetics* **154**: 95–97.
- Ashton NW, Cove DJ, Featherstone DR. 1979a.** The isolation and physiological analysis of mutants of the moss, *Physcomitrella patens*, which over-produce gametophores. *Planta* **144**: 437–442.
- Ashton NW, Grimsley NH, Cove DJ. 1979b.** Analysis of gametophytic development in the moss, *Physcomitrella patens*, using auxin and cytokinin resistant mutants. *Planta* **144**: 427–435.
- Bennett TA, Liu MM, Aoyama T, Bierfreund NM, Braun M, Coudert Y, Dennis RJ, O'Connor D, Wang XY, White CD, et al. 2014.** Plasma membrane-targeted PIN proteins drive shoot development in a moss. *Current Biology* **24**: 2776–2785.
- Bezanilla M, Pan A, Quatrano RS. 2003.** RNA Interference in the Moss *Physcomitrella patens*. *Plant Physiology* **133**: 470–474.
- Bezanilla M, Perroud P-F, Pan A, Klueh P, Quatrano RS. 2005.** An RNAi system in *Physcomitrella patens* with an internal marker for silencing allows for rapid identification of loss of function phenotypes. *Plant Biology* **7**: 251–257.
- Bolger AM, Lohse M, and Usadel B. 2014.** Trimmomatic: a flexible trimmer for Illumina sequence data. *Bioinformatics* **30**: 2114–2120.
- Chater C, Kamisugi Y, Movahedi M, Fleming A, Cuming AC, Gray JE, Beerling DJ. 2011.** Regulatory mechanism controlling stomatal behavior conserved across 400 million years of land plant evolution. *Current Biology* **21**: 1025–1029.
- Courtice GRM, Ashton NW, Cove DJ. 1978.** Evidence for the restricted passage of metabolites into

the sporophyte of the moss *Physcomitrella patens* (Hedw.) Br. Eur. *Journal of Bryology* **10**: 191–198.

Cove D, Bezanilla M, Harries P, Quatrano R. 2006. Mosses as model systems for the study of metabolism and development. *Annual Review of Plant Biology* **57**: 497–520.

Cove DJ, Perroud PF, Charron AJ, McDaniel SF, Khandelwal A, Quatrano RS. 2009a. Transformation of moss *Physcomitrella patens* gametophytes using a biolistic projectile delivery system. *Cold Spring Harbor protocols* **2009**: pdb prot5145.

Cove DJ, Perroud PF, Charron AJ, McDaniel SF, Khandelwal A, Quatrano RS. 2009b. Somatic hybridization in the moss *Physcomitrella patens* using PEG-induced protoplast fusion. *Cold Spring Harbor protocols* **2009**: pdb prot5141.

Cove DJ, Quatrano RS. 2006. Agravitropic mutants of the moss *Ceratodon purpureus* do not complement mutants having a reversed gravitropic response. *Plant, Cell & Environment* **29**: 1379–1387.

Egener T, Granado J, Guitton M-C, Hohe A, Holtorf H, Lucht JM, Rensing SA, Schlink K, Schulte J, Schween G, et al. 2002. High frequency of phenotypic deviations in *Physcomitrella patens* plants transformed with a gene-disruption library. *BMC Plant Biology* **2**: 6.

Engel PP. 1968. The Induction of Biochemical and Morphological Mutants in the Moss *Physcomitrella patens*. *American Journal of Botany* **55**: 438.

Eshed Y, Baum SF, Perea J V, Bowman JL. 2001. Establishment of polarity in lateral organs of plants. *Current Biology* **11**: 1251–1260.

Featherstone DR, Cove DJ, Ashton NW. 1990. Genetic analysis by somatic hybridization of cytokinin overproducing developmental mutants of the moss, *Physcomitrella patens*. *Molecular & General Genetics* **222**: 217–224.

Grimsley NH, Ashton NW, Cove DJ. 1977a. Complementation analysis of auxotrophic mutants of the moss, *Physcomitrella patens*, using protoplast fusion. *Molecular & General Genetics* **155**: 103–107.

Grimsley NH, Ashton NW, Cove DJ. 1977b. The production of somatic hybrids by protoplast fusion in the moss, *Physcomitrella patens*. *Molecular & General Genetics* **154**: 97–100.

Hirano K, Nakajima M, Asano K, Nishiyama T, Sakakibara H, Kojima M, Katoh E, Xiang H, Tanahashi T, Hasebe M, et al. 2007. The *GID1*-mediated gibberellin perception mechanism is conserved in the Lycophyte *Selaginella moellendorffii* but not in the Bryophyte *Physcomitrella patens*. *Plant Cell* **19**: 3058–3079.

- Horst NA, Katz A, Pereman I, Decker EL, Ohad N, Reski R. 2016.** A single homeobox gene triggers phase transition, embryogenesis and asexual reproduction. *Nature Plants* **2**: 15209.
- Horton RM, Cai Z, Ho SN, Pease LR. 2013.** Gene splicing by overlap extension: Tailor-made genes using the polymerase chain reaction. *BioTechniques* **54**: 528–535.
- Kamisugi Y, Von Stackelberg M, Lang D, Care M, Reski R, Rensing SA, Cuming AC. 2008.** A sequence-anchored genetic linkage map for the moss, *Physcomitrella patens*. *The Plant Journal* **56**: 855–866.
- Li H. 2013.** Aligning sequence reads, clone sequences and assembly contigs with BWA-MEM. arxiv.org/abs/1303.3997.
- Lu P, Han X, Qi J, Yang J, Wijeratne AJ, Li T, Ma H. 2012.** Analysis of Arabidopsis genome-wide variations before and after meiosis and meiotic recombination by resequencing Landsberg erecta and all four products of a single meiosis. *Genome Research* **22**: 508-518.
- Ludwig-Muller J, Julke S, Bierfreund NM, Decker EL, Reski R. 2009.** Moss (*Physcomitrella patens*) GH3 proteins act in auxin homeostasis. *New Phytologist* **181**: 323–338.
- McKenna A, Hanna M, Banks E, Sivachenko A, Cibulskis K, Kernytzky A, Garimella K, Altschuler D, Gabriel S, Daly M, DePristo MA. (2010).** The Genome Analysis Toolkit: A MapReduce framework for analyzing next-generation DNA sequencing data. *Genome Research* **20**: 1297-1303.
- Menand B, Yi K, Jouannic S, Hoffmann L, Ryan E, Linstead P, Schaefer DG, Dolan L. 2007.** An ancient mechanism controls the development of cells with a rooting function in land plants. *Science* **316**: 1477–1480.
- Moody LA, Kelly S, Rabbinoiwitsch E, Langdale JA. 2018.** Genetic regulation of the 2D to 3D growth transition in the moss *Physcomitrella patens*. *Current Biology* (in press).
- Mosquna A, Katz A, Decker EL, Rensing SA, Reski R, Ohad N. 2009.** Regulation of stem cell maintenance by the Polycomb protein FIE has been conserved during land plant evolution. *Development* **136**: 2433–2444.
- Nguyen AW, Daugherty PS. 2005.** Evolutionary optimization of fluorescent proteins for intracellular FRET. *Nature Biotechnology* **23**: 355.
- Nishiyama T. 2000.** Tagged Mutagenesis and Gene-trap in the Moss, *Physcomitrella patens* by Shuttle Mutagenesis. *DNA Research* **7**: 9–17.

- Perroud P-F, Cove DJ, Quatrano RS, McDaniel SF. 2011.** An experimental method to facilitate the identification of hybrid sporophytes in the moss *Physcomitrella patens* using fluorescent tagged lines. *New Phytologist* **191**: 301–306.
- Perroud P-F, Demko V, Johansen W, Wilson RC, Olsen OA, Quatrano RS. 2014.** Defective Kernel 1 (DEK1) is required for three-dimensional growth in *Physcomitrella patens*. *New Phytologist* **203**: 794–804.
- Prigge MJ, Lavy M, Ashton NW, Estelle M. 2010.** *Physcomitrella patens* auxin-resistant mutants affect conserved elements of an auxin-signaling pathway. *Current Biology* **20**: 1907–1912.
- Rensing SA, Lang D, Zimmer AD, Terry A, Salamov A, Shapiro H, Nishiyama T, Perroud PF, Lindquist EA, Kamisugi Y, *et al.* 2008.** The *Physcomitrella* genome reveals evolutionary insights into the conquest of land by plants. *Science* **319**: 64–69.
- Reski R, Frank W. 2005.** Moss (*Physcomitrella patens*) functional genomics--Gene discovery and tool development, with implications for crop plants and human health. *Brief Funct Genomic Proteomic* **4**: 48–57.
- Sakakibara K, Reisewitz P, Aoyama T, Friedrich T, Ando S, Sato Y, Tamada Y, Nishiyama T, Hiwatashi Y, Kurata T, *et al.* 2014.** WOX13-like genes are required for reprogramming of leaf and protoplast cells into stem cells in the moss *Physcomitrella patens*. *Development* **141**: 1660–1670.
- Saruhashi M, Kumar Ghosh T, Arai K, Ishizaki Y, Hagiwara K, Komatsu K, Shiwa Y, Izumikawa K, Yoshikawa H, Umezawa T, *et al.* 2015.** Plant Raf-like kinase integrates abscisic acid and hyperosmotic stress signaling upstream of SNF1-related protein kinase2. *Proceedings of the National Academy of Sciences* **112**: E6388–E6396.
- Schaefer DG, Zrýd JP. 2001.** The moss *Physcomitrella patens*, now and then. *Plant Physiology* **127**: 1430–8.
- Schaefer D, Zrýd JP, Knight CD, Cove DJ. 1991.** Stable transformation of the moss *Physcomitrella patens*. *Molecular & General Genetics* **226**: 418–424.
- von Stackelberg M, Rensing SA, Reski R. 2006.** Identification of genic moss SSR markers and a comparative analysis of twenty-four algal and plant gene indices reveal species-specific rather than group-specific characteristics of microsatellites. *BMC Plant Biology* **6**: 9.
- Stevenson SR, Kamisugi Y, Trinh CH, Schmutz J, Jenkins JW, Grimwood J, Muchero W, Tuskan GA, Rensing SA, Lang D, *et al.* 2016a.** Genetic Analysis of *Physcomitrella patens* Identifies ABSCISIC ACID NON-RESPONSIVE, a Regulator of ABA Responses Unique to Basal Land Plants

and Required for Desiccation Tolerance. *The Plant Cell* **28**: 1310–27.

Stevenson SR, Kamisugi Y, Trinh CH, Schmutz J, Jenkins JW, Grimwood J, Muchero W, Tuskan GA, Rensing SA, Lang D, et al. 2016b. Genetic Analysis of *Physcomitrella patens* Identifies ABCISIC ACID NON-RESPONSIVE, a Regulator of ABA Responses Unique to Basal Land Plants and Required for Desiccation Tolerance. *The Plant Cell* **28**: 1310–27.

Vives C, Charlot F, Mhiri C, Contreras B, Daniel J, Epert A, Voytas DF, Grandbastien M-A, Nogu   F, Casacuberta JM. 2016. Highly efficient gene tagging in the bryophyte *Physcomitrella patens* using the tobacco (*Nicotiana tabacum*) Tnt1 retrotransposon. *New Phytologist* **212**: 759–769.

Yasumura Y, Crumpton-Taylor M, Fuentes S, Harberd NP. 2007. Step-by-step acquisition of the gibberellin-DELLA growth-regulatory mechanism during land-plant evolution. *Current Biology* **17**: 1225–1230.

Yasumura Y, Moylan EC, Langdale JA. 2005. A conserved transcription factor mediates nuclear control of organelle biogenesis in anciently diverged land plants. *Plant Cell* **17**: 1894–1907.

FIGURE LEGENDS

Fig. 1. Successful somatic hybridization. **a)** Haploid protoplasts from PM-YPet (left) and NLS-GFP (right) lines. **b–d)** Diploid hybrids after somatic hybridization between PM-YPet and NLS-GFP protoplasts: NLS-GFP homodikaryon (b), PM-YPet homodikaryon (c), NLS-GFP/PM-YPet heterodikaryon (d). Arrows indicate nuclei. Asterisk shows fusion event in (c). Scale bar = 10µm.

Fig. 2. Stable synkaryons. **a)** Gd::GFP and Vx::mCherry haploid lines and a Gd::GFP/Vx::mCherry diploid line. Images show chlorophyll autofluorescence (blue), GFP (green), mCherry (red) and a merge of all three. Scale bar = 10µm. **b)** Gd::GFP/Vx::mCherry tetraploid sporophyte. Scale bar = 100µm.

Fig. 3. Phenotype of stable synkaryons. Representative images of gametophores and protonemata from Gd::GFP (a, d), Vx::mCherry (b, e) and reproductively viable Gd::GFP/Vx::mCherry diploid hybrids (c, f). Scale = 5mm (a–c) and 1mm (d–f).

Fig. 4. Density of single nucleotide variants between Gd and Vx strains. Box plots show variant density for each 10 kb window for each chromosome. Median = 35 single nucleotide variants per 10 kb window (i.e. 1 variant site per 286 b).

SUPPLEMENTARY INFORMATION

File S1 Morphology, fluorescence at different developmental stages, and transgene sequence of PM-YPet line.

File S2 Variant positions in the *P. patens* 318 v3 genome sequence.

Table 1 Antibiotic segregation of progeny derived from five independent Gd::GFP/Vx::mCherry hybrid sporophytes.

	Observed					Expected					Chi-square
	G ^R /H ^S	G ^R /H ^R	G ^S /H ^R	G ^S /H ^S	Total	G ^R /H ^S	G ^R /H ^R	G ^S /H ^R	G ^S /H ^S	Total	
Gd::GFP/Vx::mCherry-19	12	88	18	0	118	16.39	81.94	16.39	3.27	118	5.142 ***
Gd::GFP/Vx::mCherry-23	18	80	16	0	114	15.83	79.17	15.83	3.17	114	3.47 ***
Gd::GFP/Vx::mCherry-26	6	65	14	0	85	11.81	59.03	11.81	2.36	85	6.23 ***
Gd::GFP/Vx::mCherry-30	11	71	22	0	104	14.44	72.22	14.44	2.89	104	7.69 ***
Gd::GFP/Vx::mCherry-32	13	81	21	0	115	15.97	79.86	15.97	3.19	115	5.34 ***

Observed numbers are consistent with all the hybrid gametophores being diploid (based on a 5:25:5:1 segregation ratio). Abbreviated as G418 resistant (G^R), G418 susceptible (G^S), Hygromycin resistant (H^R) and Hygromycin susceptible (H^S). Chi-square P<0.005 ***, df = 3.

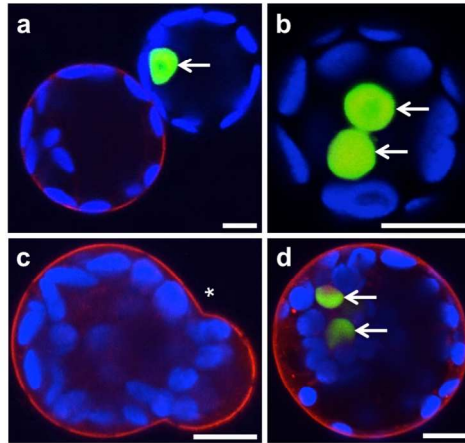


Figure 1: Successful somatic hybridization. a) Haploid protoplasts from PM-YPet (left) and NLS-GFP (right) lines. **b-d)** Dikaryons after somatic hybridization between PM-YPet and NLS-GFP protoplasts: NLS-GFP homodikaryon (b), PM-YPet homodikaryon (c), NLS-GFP/PM-YPet heterodikaryon (d). Arrows indicate nuclei. Asterisk shows fusion event in (c). Scale bar = 10µm.

Figure 1

190x253mm (225 x 225 DPI)

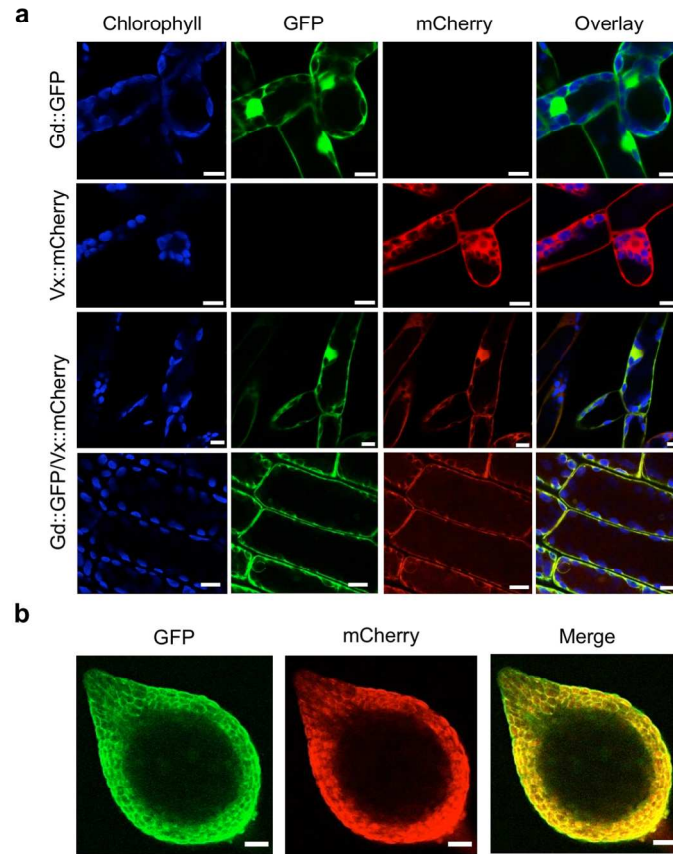


Figure 2: Stable synkaryons. a) Gd::GFP and Vx::mCherry haploid lines and a Gd::GFP/Vx::mCherry heterodikaryon. Images show chlorophyll autofluorescence (blue), GFP (green), mCherry (red) and a merge of all three. Scale bar = 10 μ m. **b)** Gd::GFP/Vx::mCherry tetraploid sporophyte. Scale bar = 100 μ m.

Figure 2

190x253mm (225 x 225 DPI)

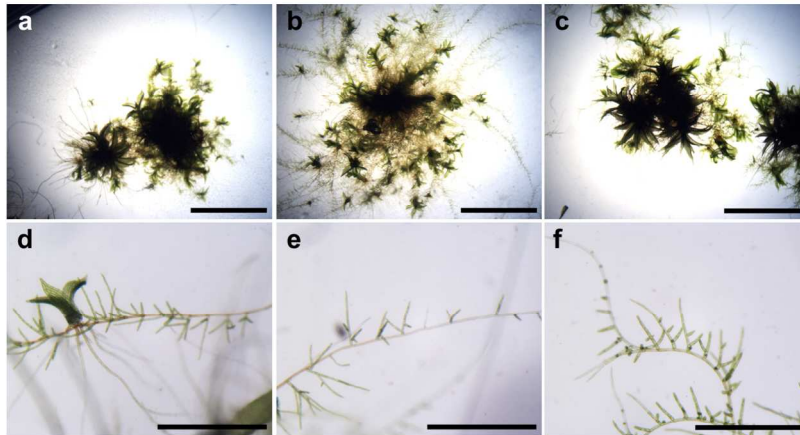


Figure 3: Phenotype of stable sinkaryons. Representative images of gametophores and protonemata from Gd::GFP (a, d), Vx::mCherry (b, e) and reproductively viable Gd::GFP/Vx::mCherry diploid hybrids (c, f). Scale = 5mm (a-c) and 1mm (d-f).

Figure 3

190x253mm (225 x 225 DPI)

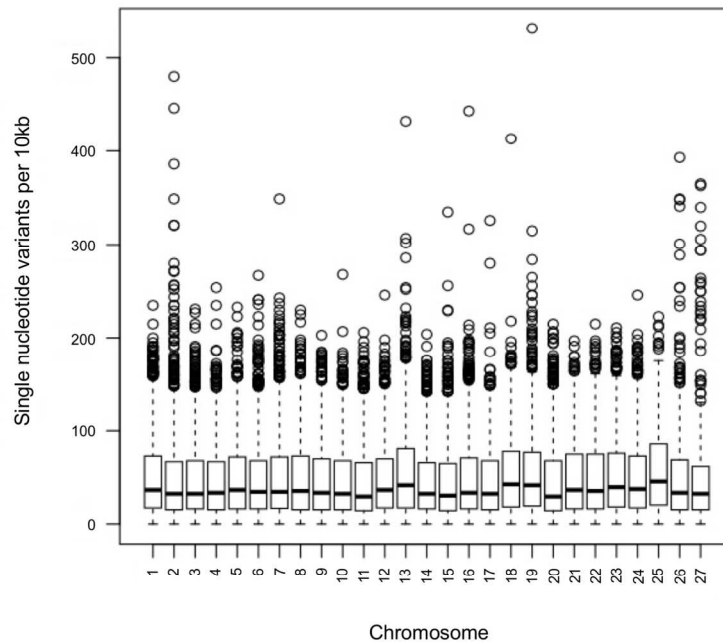


Figure 4: Density of single nucleotide variants between Gd and Vx strains. Box plots show variant density for each 10 kb window for each chromosome. Median = 35 single nucleotide variants per 10 kb window (i.e. 1 variant site per 286b).

Figure 4

253x338mm (169 x 169 DPI)